EPJ Web of Conferences **54**, 01016 (2013)
DOI: 10.1051/epjconf/20135401016

Complex photonic structures for energy efficiency

M. Burresi and D. S. Wiersma

European Laboratory for Non-linear Spectroscopy (LENS), University of Florence Via Nello Carrara 1, 50019 Sesto Fiorentino (FI), Italy

Istituo Nazionale di Ottica (CNR-INO) - Largo Fermi 6, 50125 Firenze, Italy

Summary. — Photonic structures are playing an increasingly important role in energy efficiency. In particular, they can help to control the flow of light and improve the optical properties of photovoltaic solar cells. We will explain the physics of light transport in such structures with a special focus on disordered materials.

1. – Introduction

The quest for efficient harvesting of solar radiation is extremely relevant in the renewable energy field. Research has an interdisciplinary character, ranging from material science [1-6] to optics [7,8] and nanophotonics [9-13]. Particular attention is dedicated to the so-called third-generation solar cells, among which thin-film technologies provide a promising alternative to standard silicon cells or to cells based on sometimes very expensive and rare, materials (*e.g.*, CdTe, CIGS) [4]. Due to the reduced thickness of these thin films (even below 1 μm), strategies to increase their performances can play an important role. Different approaches can be followed amongst which the design and fabrication of engineered photonic structures. This can either lead to enhanced absorption, or can reduce the amount of required material and hence reduce fabrication costs.

Nanophotonics offers interesting possibilities for improving solar cell absorption [14-16]. Standard optics is limited by an upper thermodynamical limit [17], which can however be surpassed by nanophotonic strategies in particular when the absorbing films are extremely thin [18]. Through different photonic architectures it is possible to augment the optical absorption by, for instance, trapping light within ultra-thin films [14], or even manipulate the photon density of state [15] or slowing down light in absorbing thin films. This can be achieved by periodic photonic structures [14, 15] or disordered ones [19-21], as it has been recently proposed in a two-dimensional system [22] in which disorder modes are on the verge of light (Anderson) localization [23-25].

In these proceedings we will focus on the optics of disordered systems. Disorder can slow down transport or increase the path length of light inside a material, and thus significantly increasing the probability of light to be absorbed. Different degrees of disorder can be used to control the transport. Also, different dimensions of the disordered system give rise to significantly different optical properties, providing a variety of possible strategies, depending on the specific geometries of the system.

2. – Multiple scattering for controlling light propagation

2˙1. *Coherent vs. incoherent transport.* – A photonic material in which the refractive index is modulated can have various optical properties depending on the type of modulation. In a disordered structure, light propagation is dominated by multiple scattering. In very first approximation this process can be considered as a random walk from one scattering element to another. However, this simplified description does not take into account the wave nature of light and the resulting fascinating interference effects. The arrangement and density of scattering elements can make the effects of interference dominant. For instance, ordered dielectric systems, with a lattice constant comparable to the wavelength, behave as a crystal for light waves. When the scattering strength is high enough a photonic bandgap is expected to occur [26, 27]. On the other hand, light waves in disordered materials undergo random multiple scattering, that to first order, by averaging over different realizations of disorder, can be described as a diffusive type of transport. What makes disordered systems interesting is that interference effects can survive the random multiple scattering. Interference of light in random dielectric systems influences the transport in a way that is similar to the interference that occurs for electrons when they propagate in disordered conducting materials. As a result, light propagation in disordered systems shows many similarities with the propagation of electrons in (semi)conductors. Various phenomena that are common for electron transport have now also been found to exist for light waves [28]. Important examples are weak localization [29], the photonic Hall effect [30], optical magneto resistance [31], Anderson localization [32], Bloch oscillations and Zener tunneling [33, 34], and universal conductance fluctuations [35]. In the case of Anderson localization the interference effects are so strong that the transport comes to a halt and the light becomes localized in randomly distributed modes inside the system.

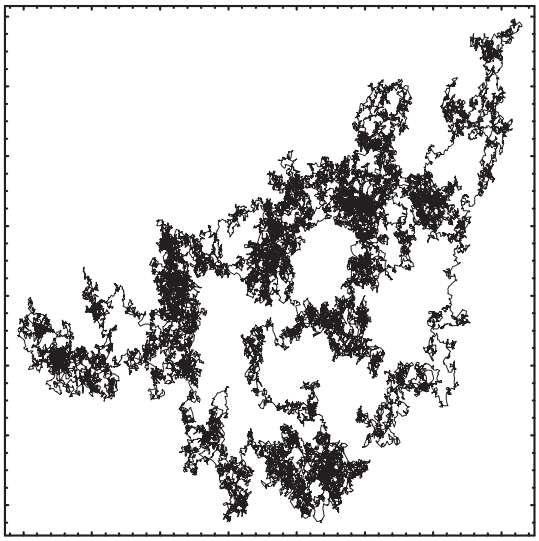

Fig. 1. – Gaussian random walk (Brownian) obtained by Monte Carlo simulation in the absence of absorption. The multiple-scattering process slows down the transport of the walker (light) in the medium with respect the homogenous scatterer-free material. This in turn induces an increase of the optical thickness of the system.

By engineering the distribution of scattering elements, control on light propagation can be achieved, with great use for photovoltaic applications. In particular, light can be slowed down in the material increasing the probability of light-matter interaction. As a consequence light can be "held" in the material longer that it would do in its homogeneous counterpart experiencing an effectively thicker material. This could be of paramount importance for photovoltaic applications, for which the reduction of material use, for economical and technical reasons, is constantly pursed.

2˙2. *Disordered structures and random walks.* – Disordered materials can be created in a variety of ways, amongst which one of the most simple ways maybe that of grinding solids into fine powders. Alternative approaches include etching of glasses or semiconductors such as silicon [36] and gallium phosphide [37]. For photovoltaic application the fabrication of disorder material has to be handled with a certain care. The quality of the atomic structure has to be extremely good in order to avoid the occurrence of defect sates in the electronic band structure, ensuring a good electronic transport.

As mentioned above, light propagation in disordered materials can be described in first approximation as a random walk process, analogous to the Brownian motion of particles in a fluid [38]. Having scattering elements homogeneously distributed in space generally leads to a diffusive type of transport. In such a regime, light transport is often studied by means of Monte Carlo simulations, in which certain assumptions on the function describing the distribution of step-length between two scattering events have to

be made. Normally, the step length distribution has finite moments which unequivocally leads, due to the Central-Limit Theorem, to a normal distribution of the step size and to a Brownian-like transport (fig. 1), which in turn can be described by diffusion theory (see next section). The multiple scattering process significantly slows down the propagation of light and thus increasing the probability of absorption. The effect of absorption on light transport can be implemented easily in Monte Carlo simulations by adding a certain probability P_a to be absorbed at each step, following the well-known Lambert-Beer's law $P_a = e^{-\alpha s}$, where s is the step length and α is the absorption coefficient of the material in which the multiple scattering occurs.

3. – Diffusion theory

In the following sections we will describe the theoretical basis that is often used to model light transport in random media. Before considering interference, our starting point is that of diffusive transport. In the diffusion approximation, the propagation of the intensity is described as a random walk with a characteristic mean free path ℓ. Only the intensity and not the electric field itself is considered, so the wave character of the light is not taken into account. Usually also the vector nature of light is disregarded. In reality, there are two polarization channels over which light is distributed in the scattering process. In practise though, often good agreement can be found between scalar diffusion theory and experimental data for light backscattered from a disordered sample when the appropriate polarization channels are considered. A typical diffusion equation for the intensity $I(\boldsymbol{r}, t)$ can be written as follows [39]:

$$\frac{\partial I(\boldsymbol{r},t)}{\partial t} = D\nabla^2 I(\boldsymbol{r},t) - \frac{v}{\ell_{\mathrm{i}}} I(\boldsymbol{r},t), \tag{3.1}$$

where D is the Boltzmann diffusion constant, which, in case of an exponential step-length distribution is given by $D = \frac{1}{3}\ell v$, with ℓ the transport mean free path (see below), v is the transport velocity for the light inside the medium, and ℓ_{i} is the inelastic mean free path. Note that a proper definition of the intensity in terms of the electric field will be given in sect. **4**, where we will deal with multiple scattering and include interference effects. The diffusion equation as written above is used now to introduce some basic concepts.

3˙1. *Important length scales for diffusive systems.* – The characteristic length scales relevant for the scattering of the light, are the transport mean free path ℓ and the scattering mean free path ℓ_{s}. The scattering mean free path is defined as the average distance between two scattering events. For a random distribution of small particles, ℓ_{s} is given by

$$\ell_{\mathrm{s}} = \frac{1}{n\sigma_{\mathrm{sc}}}\,, \tag{3.2}$$

with n the density of the scattering particles and $\sigma_{\rm sc}$ their scattering cross-section. The transport mean free path ℓ is defined as the average distance the light travels from some arbitrary point A in the sample, before its memory of direction of propagation it had at A is lost. For isotropic scattering, ℓ is equal to $\ell_{\rm s}$. For anisotropic scattering, and if Anderson localization effects can be neglected, the transport mean free path ℓ is given by

$$\ell = \frac{1}{1 - \langle \cos\theta \rangle} \frac{1}{n\sigma_{\rm sc}}, \tag{3.3}$$

where $\langle \cos\theta \rangle$ is the average cosine of the scattering angle for one scatterer.

4. – Interference effects: transport beyond diffusion

In the diffusion approximation we are missing a fundamental aspect of light transport, namely that of interference between multiply scattered waves. To take that into account properly we have to develop a transport theory that considers the multiple scattering of the electric field instead of the intensity, in such a way that none of the phase information is lost. Starting point is the set of Maxwell's equations for the electric and magnetic field. Green's function theory is then used to derive perturbation expansions both for the electric field and the intensity.

Starting from Maxwell's equations, the electric field can be shown to fulfill the time-dependent wave equation [40]:

$$\nabla^2 \mathbf{E}(\boldsymbol{r}, t) + \boldsymbol{\nabla} \frac{\mathbf{E}(\boldsymbol{r}, t) \cdot \boldsymbol{\nabla} \epsilon(\boldsymbol{r})}{\epsilon(\boldsymbol{r})} - \frac{\epsilon(\boldsymbol{r})}{c_0^2} \frac{\partial^2 \mathbf{E}(\boldsymbol{r}, t)}{\partial t^2} = 0. \tag{4.4}$$

The second term in this equation, containing the gradient of $\epsilon(\boldsymbol{r})$, is zero in regions of space where $\epsilon(\boldsymbol{r})$ is constant. We will regard a collection of particles with a constant refractive index in a surrounding medium with another constant refractive index, so $\epsilon(\boldsymbol{r})$ is constant inside and outside the particles. In that case, the second term in eq. (4.4) determines the boundary condition for the electric field at the particle boundary, and is zero elsewhere. By using a Fourier transformation with respect to time, the explicit time dependence in eq. (4.4) can be removed, and all harmonics of the resulting Fourier representation will follow the time-independent Helmholtz equation:

$$\nabla^2 E(\boldsymbol{r}) + (\omega/c_0)^2 \epsilon(\boldsymbol{r}) E(\boldsymbol{r}) = 0, \tag{4.5}$$

where $E(\boldsymbol{r})$ denotes one of the field components of the electric field, inside or outside the scatterers. The same equation holds for the magnetic field components. Here $\epsilon(\boldsymbol{r})$ is the (random) place-dependent dielectric constant of the system, ω the frequency of the electric field, and c_0 the vacuum speed of light. The wave equation can be written as

$$\nabla^2 E(\boldsymbol{r}) + (\omega/c_0)^2 E(\boldsymbol{r}) = V(\boldsymbol{r}) E(\boldsymbol{r}), \tag{4.6}$$

where $V(\boldsymbol{r})$ is the scattering potential defined as $V(\boldsymbol{r}) \equiv -(\omega/c_0)^2\,[\epsilon(\boldsymbol{r}) - 1]$. For a collection of point-like scatterers with polarizability α_0, in a surrounding medium with dielectric constant 1, the scattering potential is given by

$$V(\boldsymbol{r}) = -\alpha_0(\omega/c_0)^2 \sum_i \delta(\boldsymbol{r} - \boldsymbol{r}_i), \tag{4.7}$$

with $\boldsymbol{r}_i$ the positions of the scatterers. For a subwavelength scatterer of spherical shape with dielectric constant ϵ_1 and radius a in vacuum, the polarizability is given by $\alpha_0 = a^3(\epsilon_1 - 1)/(\epsilon_1 + 2)$. Introducing the Green's function $G_0(\boldsymbol{r}_1, \boldsymbol{r}_2)$ as the solution of

$$\nabla^2 G_0(\boldsymbol{r}_1, \boldsymbol{r}_2) + (\omega/c_0)^2 G_0(\boldsymbol{r}_1, \boldsymbol{r}_2) = -\delta(\boldsymbol{r}_1 - \boldsymbol{r}_2), \tag{4.8}$$

one can write the solution to eq. (4.6) formally as

$$E(\boldsymbol{r}_1) = E_{\rm in}(\boldsymbol{r}_1) - \int \mathrm{d}\boldsymbol{r}_2\, G_0(\boldsymbol{r}_1, \boldsymbol{r}_2) V(\boldsymbol{r}_2) E(\boldsymbol{r}_2), \tag{4.9}$$

where $E_{\rm in}(\boldsymbol{r}_1)$ is a solution of the homogeneous wave equation obtained by taking $V(\boldsymbol{r}) = 0$ in eq. (4.6). $E_{\rm in}(\boldsymbol{r}_1)$ represents the incoming coherent wave. $G_0(\boldsymbol{r}_1, \boldsymbol{r}_2)$ is also referred to as the bare Green's function and describes the propagation of the field in a medium without scatterers. It is given by

$$G_0(\boldsymbol{r}_1, \boldsymbol{r}_2) = \frac{e^{-ik|\boldsymbol{r}_1 - \boldsymbol{r}_2|}}{4\pi|\boldsymbol{r}_1 - \boldsymbol{r}_2|}\,, \tag{4.10}$$

with $k = \omega/c_0$. By iterating the recursion relation eq. (4.9), one obtains the following perturbation series for the electric field:

$$\begin{aligned} E(\boldsymbol{r}_1) = E_{\rm in}(\boldsymbol{r}_1) &- \int \mathrm{d}\boldsymbol{r}_2\; G_0(\boldsymbol{r}_1, \boldsymbol{r}_2) V(\boldsymbol{r}_2) E_{\rm in}(\boldsymbol{r}_2) \\ &+ \iint \mathrm{d}\boldsymbol{r}_2 \mathrm{d}\boldsymbol{r}_3\; G_0(\boldsymbol{r}_1, \boldsymbol{r}_2) V(\boldsymbol{r}_2) G_0(\boldsymbol{r}_2, \boldsymbol{r}_3) V(\boldsymbol{r}_3) E_{\rm in}(\boldsymbol{r}_3) \\ &- \iiint \mathrm{d}\boldsymbol{r}_2 \ldots \mathrm{d}\boldsymbol{r}_4\, G_0(\boldsymbol{r}_1, \boldsymbol{r}_2) V(\boldsymbol{r}_2) G_0(\boldsymbol{r}_2, \boldsymbol{r}_3) V(\boldsymbol{r}_3) G_0(\boldsymbol{r}_3, \boldsymbol{r}_4) V(\boldsymbol{r}_4) E_{\rm in}(\boldsymbol{r}_4) + \cdots\,, \end{aligned} \tag{4.11}$$

where all integrals are taken over the volume of the sample. The above expression depends on $E_{\rm in}$. To describe the propagation of the field in the medium independently of $E_{\rm in}$, we use the total Green's function $G(\boldsymbol{r}_1, \boldsymbol{r}_2)$ which is defined as the solution of

$$\nabla^2 G(\boldsymbol{r}_1, \boldsymbol{r}_2) + (\omega/c_0)^2 \epsilon(\boldsymbol{r}) G(\boldsymbol{r}_1, \boldsymbol{r}_2) = -\delta(\boldsymbol{r}_1 - \boldsymbol{r}_2). \tag{4.12}$$

The Green's function $G(\boldsymbol{r}_1, \boldsymbol{r}_2)$ describes the field at any point $\boldsymbol{r}_1$ in the medium, due to a source at $\boldsymbol{r}_2$. The perturbation series for $G(\boldsymbol{r}_1, \boldsymbol{r}_2)$ is

$$G(\boldsymbol{r}_1, \boldsymbol{r}_2) = G_0(\boldsymbol{r}_1, \boldsymbol{r}_2) - \int \mathrm{d}\boldsymbol{r}_\mathrm{a} G_0(\boldsymbol{r}_1, \boldsymbol{r}_\mathrm{a}) V(\boldsymbol{r}_\mathrm{a}) G_0(\boldsymbol{r}_\mathrm{a}, \boldsymbol{r}_2) + \iint \mathrm{d}\boldsymbol{r}_\mathrm{a} \mathrm{d}\boldsymbol{r}_\mathrm{b} G_0(\boldsymbol{r}_1, \boldsymbol{r}_\mathrm{a}) V(\boldsymbol{r}_\mathrm{a}) G_0(\boldsymbol{r}_\mathrm{a}, \boldsymbol{r}_\mathrm{b}) V(\boldsymbol{r}_\mathrm{b}) G_0(\boldsymbol{r}_\mathrm{b}, \boldsymbol{r}_2) - \cdots . \tag{4.13}$$

Note that $V(\boldsymbol{r})$ (given by eq. (4.7)) contains the contributions from all scatterers. The first term of (4.13) describes propagation without scattering, the second term equals the sum of all single scattering contributions, the third term the sum of all double-scattering contributions, etc. To simplify the notation often Feynman-type scattering diagrams are used [38]. With such a diagrammatic notation it is easier to notice the occurrence of *recurrent scattering events*. These are events in which a wave is scattered by a specific scatterer, scattered by at least one other scatterer and then returns to this specific scatterer again. For relatively weak scattering (diluted systems), recurrent scattering events can be neglected. This is the so-called *independent scattering approximation* in which the presence of other scatterers does not influence a single scattering. In a denser system (strong scattering) the recurrent scattering events have a more relevant contribution, but the nature of the transport remain diffusive [38].

The total Green's function $G(\boldsymbol{r}_1, \boldsymbol{r}_2)$ depends on the positions of the scatterers, requiring to know exactly the distribution of the scatterers to infer the transport properties of the systems. A useful quantity is the averaged or "dressed" Green's function $G(\boldsymbol{r}_1 - \boldsymbol{r}_2)$, which is obtained by averaging $G(\boldsymbol{r}_1, \boldsymbol{r}_2)$ over the positions of the scatterers. When the distribution of scatterers is truly randomized the phase of the scattered field averaged out, thus significantly simplifying the problem([1]). In the self-avoiding multiple-scattering approximation $G(\boldsymbol{r}_1 - \boldsymbol{r}_2)$ can be calculated from (4.13), by Fourier transforming to momentum space. In momentum space the summation can be performed and after transforming back to real space one finds

$$G(\boldsymbol{r}_1 - \boldsymbol{r}_2) \equiv \langle G(\boldsymbol{r}_1, \boldsymbol{r}_2) \rangle = \frac{e^{-iK|\boldsymbol{r}_1 - \boldsymbol{r}_2|}}{4\pi|\boldsymbol{r}_1 - \boldsymbol{r}_2|}, \tag{4.14}$$

where $K = \sqrt{(\omega/c_0)^2 + nt}$ is the (complex) effective k-vector for the light inside the sample, with n the density of scatterers.

Given the complexity of measuring fields at optical frequencies it is very useful to move from the field propagator to the intensity propagator. The intensity is defined as the energy that crosses a unit area per unit of time. It is given by the magnitude of the

([1]) In the case of a not purely random system, such as correlated (amorphous) disorder, the average is not enough to cancel out the phase relation between the scattered fields and a certain degree of coherence is conserved, leading to a rich spectral response.

cycle average of the Poynting vector $\mathbf{E} \times \mathbf{B}$, which can be written as

$$I(\boldsymbol{r}) = \frac{c_0\, n}{2} |\mathbf{E}(\boldsymbol{r})|^2, \tag{4.15}$$

with c_0 the vacuum speed of light, and n the refractive index of the medium. In terms of the total Green's function $G(\boldsymbol{r}_1, \boldsymbol{r}_2)$, the intensity is given by

$$I(\boldsymbol{r}) \equiv \frac{c_0\, n}{2} E(\boldsymbol{r}) E^*(\boldsymbol{r}) = \frac{c_0\, n}{2} \iint \mathrm{d}\boldsymbol{r}_1 \mathrm{d}\boldsymbol{r}_2 G(\boldsymbol{r}\,, \boldsymbol{r}_1) G^*(\boldsymbol{r}\,, \boldsymbol{r}_2) E_{\mathrm{in}}(\boldsymbol{r}_1) E^*_{\mathrm{in}}(\boldsymbol{r}_2), \tag{4.16}$$

where $G(\boldsymbol{r}_1, \boldsymbol{r}_2)$ is the unaveraged Green's function. The product $G\,G^*$ describes the intensity at any point in the system due to the product of incoming waves $E_{\mathrm{in}} E^*_{\mathrm{in}}$.

In the independent scattering approximations and applying the average over different realization of disorder, transport of intensity can be described by the average propagator $\langle G\,G^* \rangle$. Exploiting once again the Feynman diagrams it is possible to show that $\langle G\,G^* \rangle$ is mostly described by two type of diagrams: the so-called "ladder" diagrams L and "most-crossed" diagrams C [41]. The ladder diagrams describe incoherent transport of the intensity while the most-crossed diagrams describe an interference phenomenon called coherent backscattering, which is explained in the next section.

4˙1. *Weak localization.* – Maybe the most robust of interference phenomena in multiple scattering is that of weak localization [42] which originates from the fundamental concept of reciprocity. In weak localization, interference leads to a net reduction of light transport similar to the weak localization phenomenon for electrons in disordered (semi)conductors and often seen as the precursor to Anderson (or strong) localization of light [43]. Weak localization of light can be observed since it manifests itself as an enhancement of the light intensity in the exact backscattering direction. This enhancement is called the cone of coherent backscattering. Since the first experimental observation of coherent backscattering from colloidal suspensions [42], the phenomenon has been successfully studied in strongly scattering powders [44, 45], cold atom gases [46], semiconductor microcavities [47], two-dimensional random systems of rods [48], randomized laser materials [49], disordered liquid crystals [50, 51], and even photonic crystals [52].

The backscattered intensity is usually described in terms of a bistatic coefficient γ (or albedo), defined as the observed scattered flux per solid angle and per unit of observed area of the sample at normalized incident flux. This coefficient is in relation with the return probability of a photon, which is, the probability that the light path in a random walk comes back at its starting point [38]. In terms of the average scattered intensity $\langle I(\boldsymbol{r}) \rangle$ and incident intensity I_0, the bistatic coefficient can be written as

$$\gamma = \frac{4\pi r^2}{A} \frac{\langle I(\boldsymbol{r}) \rangle}{I_0}\,, \tag{4.17}$$

with A the observed area of the sample and r the distance from observer to sample.

It is convenient to separate the total bistatic coefficient $\gamma_{\rm t}$ into the contribution from most-crossed diagrams $\gamma_{\rm c}$ and from ladder diagrams, with the latter further separated into the single scattering contribution $\gamma_{\rm s}$ and multiple scattering contribution γ_ℓ:

$$\gamma_{\rm t} = \gamma_{\rm s} + \gamma_\ell + \gamma_{\rm c}. \tag{4.18}$$

By making use of the propagator described in the previous paragraph, the bistatic coefficients can be calculated as, for single scattering:

$$\gamma_{\rm s}(\theta_{\rm s}) = \frac{\mu_{\rm s}}{1+\mu_{\rm s}}\left[1 - e^{-L\kappa_{\rm e}(1+\mu_{\rm s}^{-1})}\right], \tag{4.19}$$

for the multiple scattering ladder diagrams (describing the diffuse background):

$$\gamma_\ell(\theta_{\rm s}) = \frac{3}{2\ell^3\alpha\sin[\alpha(L+2z_0)]}\,\frac{Z_1(1+e^{-2\,uL}) + Z_2(1-e^{-2\,uL}) + Z_3 e^{-L(v+u)}}{u[(u^2-\alpha^2)^2 + v^2(v^2-2\alpha^2-2u^2)]} \tag{4.20}$$

with

$$\begin{aligned} Z_1 = {} & u\,(u^2-v^2-\alpha^2)\cos[\alpha(L+2z_0)] + u\,(v^2-u^2-\alpha^2)\cos(\alpha L) \\ & +2uv\alpha\sin[\alpha(L+2z_0)] + uv\alpha\,\frac{v^2-\alpha^2-3u^2}{u^2-\alpha^2}\sin(\alpha\,L), \end{aligned} \tag{4.21}$$

$$\begin{aligned} Z_2 = {} & v\,(v^2-u^2-\alpha^2)\cos[\alpha(L+2z_0)] + 2u^2\alpha\sin(\alpha\,L) \\ & -\alpha\,(u^2+v^2-\alpha^2)\sin[\alpha(L+2z_0)] + u^2 v\,\frac{u^2-v^2+3\alpha^2}{u^2-\alpha^2}\cos(\alpha\,L), \end{aligned} \tag{4.22}$$

$$Z_3 = 2u\,(u^2-v^2+\alpha^2) + 2u\,(v^2-u^2+\alpha^2)\cos(2z_0\,\alpha) - 4uv\alpha\sin(2z_0\,\alpha), \tag{4.23}$$

and for the most-crossed diagrams (describing interference):

$$\begin{aligned} \gamma_{\rm c}(\theta_{\rm s}) = {} & \frac{3e^{-uL}}{2\ell^3\alpha\sinh[\alpha(L+2z_0)]}\,\frac{1}{(\alpha^2+\eta^2+u^2)^2-(2\alpha\eta)^2} \\ & \times\big[-2(\alpha^2+\eta^2+u^2)\cosh(2\alpha z_0)\cos(L\eta) - 4\alpha\eta\sinh(2\alpha z_0)\sin(L\eta) \\ & +2\frac{\alpha}{u}(-\alpha^2+\eta^2-u^2)\sinh(\alpha(L+2z_0))\sinh(uL) \\ & -2(\alpha^2-\eta^2-u^2)\cos(L\eta) + 2(\alpha^2+\eta^2+u^2)\cosh(\alpha(L+2z_0))\cosh(uL) \\ & +4\alpha u\sinh(\alpha L)\sinh(uL) - 2(-\alpha^2+\eta^2+u^2)\cosh(\alpha L)\cosh(uL)\big]\,. \end{aligned} \tag{4.24}$$

In these expressions, the angular dependence is determined by the following parameters: $\eta \equiv k(1-\mu_{\rm s})$, $u \equiv \frac{1}{2}\kappa_{\rm e}(1+\mu_{\rm s}^{-1})$, $v \equiv \frac{1}{2}\kappa_{\rm e}(1-\mu_{\rm s}^{-1})$, and $\alpha \equiv \sqrt{\ell_{\rm abs}^{-2} + q_\perp^2}$ with $q_\perp = k\sin\theta$.

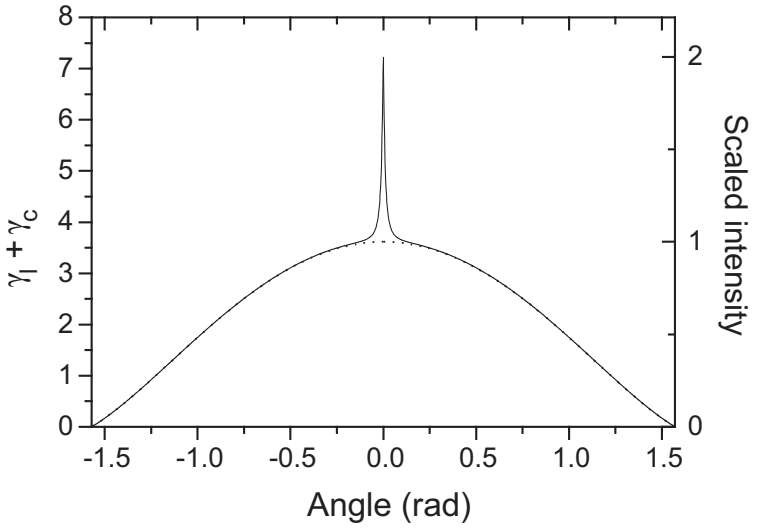

Fig. 2. – Total bistatic coefficient *versus* scattering angle, calculated in the diffusion approximation for a non-absorbing semi-infinite disordered sample with mean free path $\ell = 5\,\mu$m. Wavelength $\lambda = 700\,$nm. Scattering angle zero corresponds to exact backscattering. The dashed line is γ_ℓ, describing the diffuse background intensity. Dashed and solid lines largely overlap, except in and around exact backscattering where a narrow coherent backscattering cone is present.

As mentioned before, $\mu_\mathrm{s} = \cos\theta$, with θ the angle between the outgoing wave vector $\boldsymbol{k}_\mathrm{s}$ and $\hat{z}$, L is the sample thickness, $z_0 = 0.7104\ell$, and κ_e is the extinction coefficient given by $\kappa_\mathrm{e} = \ell_\mathrm{s}^{-1} + \ell_\mathrm{i}^{-1}$. In the limit $L \to \infty$ (*i.e.* for a semi-infinite slab), the expression for γ_c reduces to

$$\gamma_\mathrm{c}(\theta_\mathrm{s}) = \frac{3}{2\ell^3\alpha u}\,\frac{\alpha + u(1 - e^{-2\alpha z_0})}{(u+\alpha)^2 + \eta^2}\,. \tag{4.25}$$

The physical interpretation of γ_ℓ and γ_c is the following. γ_ℓ describes the (incoherent) backscattered intensity due to diffusion without interference. Its angular dependence is weak (see dashed line fig. 2): it decreases slowly at larger angles. This angular dependence is due to the fact that under larger outgoing angles, the light travels through a larger part of the sample, having a larger chance to be scattered or absorbed. The intensity described by γ_c originates from interference between reciprocal waves([2]). Because a random dielectric system obeys reciprocity, any partial wave that propagates over some distance through the sample and then leaves the illuminated area in the backscattering

([2]) Optical measurements on linear physical systems obey the general principal of reciprocity, *i.e.* their results are invariant with respect to an interchange of source and detector. In the case of a conservative system, reciprocity is equivalent to time-reversal symmetry.

direction will have a counterpropagating counterpart that follows the same path in the opposite direction. These counterpropagating partial waves have travelled over the same distance in the sample and interfere therefore constructively in the backscattering direction. This is what is described by the most-crossed diagrams. The angular dependence of γ_c is strong: it decays rapidly moving away from the exact backscattering direction (see solid line fig. 2). Away from exact backscattering, a phase difference develops between the counterpropagating waves that depends on the relative orientation of the points where the waves leave the sample. For the ensemble of light paths, the relative phases will therefore gradually randomize. After averaging over all light paths, this leads to the cone of enhanced backscattering described by γ_c [38].

Given the relation between the bistatic coefficient and the return probability, we immediately infer (fig. 2) that the probability of return to the origin is twice as large as what one would expect from diffusion theory, due to the interference effect. As the scattering strength increases, the cone becomes larger, and thus the probability that the light paths bends back increases with respect to diffusion.

4˙2. *Strong localization.* – The most surprising of interference phenomena in random systems is that of Anderson localization, which was originally discovered for electron transport. In Anderson localization of light, diffusion comes to a halt due to interference([3]). When the scattering strength of a material is increased (and hence ℓ further decreased), a phase transition into an Anderson localized state is expected to occur at $k\ell \leq 1$, with k the wave vector of the light [32,54]. For $k\ell > 1$ the transport is diffusive, which is the case in most of the available disordered dielectric materials.

Ideally such reduction of transport could be exploited for photovoltaic applications. Strong localization of light in 3D random systems requires, however, very strong scattering and, although some experimental evidence of its existence has been shown [32], no direct observation of this phenomena for 3D systems has been reported so far. Nevertheless, in order to obtain an significant enhancement of the absorption, it should be enough to work at the transition threshold, the so-called *mobility edge*. It has been predicted, but yet not experimentally proven, that for strong enough scattering strength, close to the localized regime, transport is slow down so much that light absorption significantly increases [55].

The phenomenon can be studied also in lower-dimensional systems like random dielectric multi-layers (1D) [56-58], see fig. 3a, or random holes distribution in thin films (2D) [25], see fig. 4a. One and two-dimensional optical systems have the advantage that, for large enough samples, localization always sets in (fig. 3b and 4b). That is, there is no phase transition as described above for 3D systems and transport is dominated by localized modes independently of the amount of disorder.

To what extent Anderson localization can help for absorption enhancement is still

([3]) The shape of the coherent backscattering cone described in the previous section is very sensitive to strong localization effects and can be used to map the proximity of an Anderson localization transition [53].

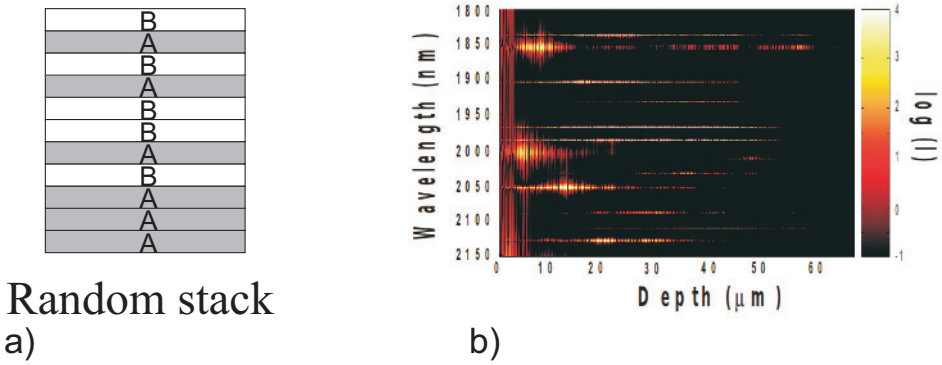

Fig. 3. – a) One-dimensional disordered photonic systems. By stacking two types of layers (A and B have e different refractive index), one can obtain a random one-dimensional structure. b) Energy distribution in a random system. Anderson localized modes occur as resonances randomly distributed along the system and at random frequencies. Localized modes can also couple into de-localized or necklace modes, that extend over the whole structure.

under investigation. Three-dimensional systems in which light unequivocally localized are still to be discovered and thus possible applications can only be hypothetical. Much more promising are 2D structures [22], for which disorder photonic media can fabricated with techniques compatible with state-of-the-art solar cells fabrication methods.

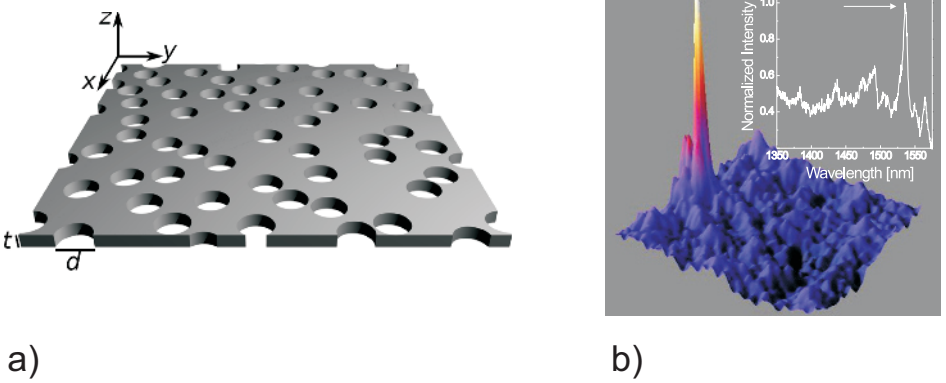

Fig. 4. – Schematic view of the randomly nanostructured film: by varying the thickness of the film and of the holes diameter the optical properties can be tuned at the frequency of interest. b) Three-dimensional view of the intensity distribution measured on a 2D disordered systems as in (a) of a localized modes. The spatial extent of this mode is around 1.4 μm at wavelength 1.5 μm. The inset shows the spectrum recorded in the position where the mode has maximum intensity.

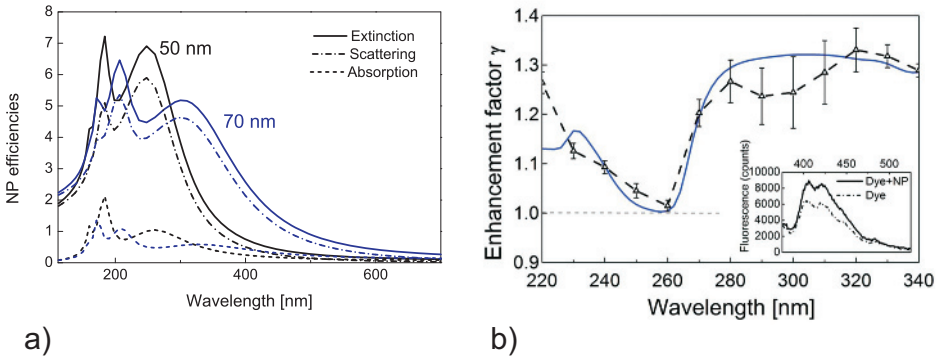

Fig. 5. – a) Extinction SCS, scattering SCS and absorption SCS of aluminum nanoparticles of 50 nm and 70 nm of diameter. b) Measured and calculated absorption enhancement of a suspension of such an aluminum nanoparticle in dye.

5. – Alternative photonic strategies

So far we have been dealing with disordered system made out of dielectric materials. However, in the last decade an increasing interest for metal-dielectric nanostructures to exploit for photovoltaic applications is developing [59]. The advantage of using metallic scattering elements is primarily due to complex permittivity of the constituent materials (*e.g.*, gold, silver, aluminum, etc.) which has a two-fold consequence on the optical response of the nano-object: i) the optical properties are often resonant, allowing to select a certain spectral range, and ii) a huge field enhancement close to the object surface can occur, increasing tremendously the light matter interaction in the vicinity of the object. Both effects are due to a coupled state between the electrons bound to the metal and the impinging electromagnetic wave, the so-called *plasmon polariton* [60]. Also in this case the photonic structure can be periodic (*e.g.*, nanostructured backreflectors [61] or arrays of nanoparticles [62]), or disordered (*e.g.*, disordered arrays [63] or suspensions of metallic nanoparticles [64]). In fig. 5a the calculated extinction, scattering and absorption cross-sections (SCS) for aluminum nanoparticles of diameter 50 nm and 70 nm is shown [64]. The choice of the radius and material employed has been made to obtain a resonant effect of the scattering properties to harvest the UV region of the solar radiation. In this way a suspension of these particles in an absorbing medium increases the optical path of the UV radiation, as shown by the measured and calculated absorption enhancement in fig. 5b, leaving almost unperturbed the propagation of light at different frequencies.

6. – Conclusions

Nanophotonics provides a great variety of solutions for increasing light-matter interaction which can be exploited to improve the performance of the absorbing materials of which we have discussed only few examples. Engineering disorder was one of the first

approaches used with this intent [17] and still its application in the photovoltaic field is vastly studied. Due to the optical "robustness" it can provide, the broadband response and the possibility to grow cheap structures, it is interesting to study disordered architectures for future implementation in new generation of solar cells.

* * *

This work was financially supported by the European community via the NoE on Nanophotonics for Energy.

REFERENCES

[1] Schaller R. D., Sykora M., Pietryga J. M. and Klimov V. I., *Nano Lett.*, **6** (2006) 424.
[2] Zahler J. M. *et al.*, *App. Phys. Lett.*, **91** (2007) 012108.
[3] Granqvist C. G., *Sol. Energ. Mater. Sol. C*, **91** (2007) 1529.
[4] Brown G. and Wu J., *Laser Photon. Rev.*, **3** (2009) 394.
[5] Chen H. *et al.*, *Nat. Photon.*, **3** (2009) 649.
[6] Krebs F. C., *Sol. Energ. Mater. Solar C*, **93** (2009) 394.
[7] Andreev V. M. *et al.*, *Sol. Energ. Mater. Sol. C*, **84** (2004) 17.
[8] Spinelli P., Verschuuren M. and Polman A., *Nat. Commun.*, **3** (2012) 692.
[9] Han S. E. and Chen G., *Nano Lett.*, **10** (2010) 1012.
[10] Atwater H. A. and Polman A., *Nat. Mater.*, **9** (2010) 205.
[11] Ferry V. E. *et al.*, *Nano Lett.*, **11** (2011) 4239.
[12] Meng X. *et al.*, *Sol. Energ. Mater. Solar C*, **95,** *Suppl.* **1** (2011) S32.
[13] Mallick S. B. *et al.*, *App. Phys. Lett.*, **100** (2012) 053113.
[14] Yu Z., Raman A. and Fan S., *Proc. Natl. Acad. Sci. U.S.A.*, **107** (2010) 17491.
[15] Callahan D. M., Munday J. N. and Atwater H. A., *Nano Lett.*, **12** (2012) 214.
[16] Bozzola A., Liscidini M. and Andreani L. C., *Opt. Express*, **20** (2012) A224.
[17] Yablonovitch E., *J. Opt. Soc. Am. A*, **72** (1982) 899.
[18] Yu Z., Raman A. and Fan S., *Phys. Rev. Lett.*, **109** (2012) 173901.
[19] Rockstuhl C., Fahr S., Bittkau K., Beckers T., Carius R., Haug F.-J., Söderström T., Ballif C. and Lederer F., *Opt. Express*, **18** (2010) 335.
[20] Martins E. R., Li J., Liu Y., Zhou J. and Krauss T. F., *Phys. Rev. B*, **86** (2012) 041404.
[21] Oskooi A., Favuzzi P. A., Tanaka Y., Shigeta H., Kawakami Y. and Noda S., *App. Phys. Lett.*, **100** (2012) 181110.
[22] Vynck K., Burresi M., Riboli F. and Wiersma D. S., *Nat. Mater.* (2012).
[23] Sigalas M. M., Soukoulis C. M., Chan C.-T. and Turner D., *Phys. Rev. B*, **53** (1996) 8340.
[24] Vanneste C. and Sebbah P., *Phys. Rev. A*, **79** (2009) 041802.
[25] Riboli F. *et al.*, *Opt. Lett.*, **36** (2011) 127.
[26] Yablonovitch E., *Phys. Rev. Lett.*, **58** (1987) 2059; John S., *Phys. Rev. Lett.*, **58** (1987) 2486.
[27] Soukoulis C. M. (Editor), *Photonic Bandgap Materials* (Kluwer, Dordrecht) 1996; Joannopoulos J. D., Meade R. D. and Winn J. N., *Photonic Crystals* (Princeton University Press, Princeton, NJ) 1995.
[28] See for instance: Sheng P., *Introduction to Wave Scattering, Localization, and Mesoscopic Phenomena* (Academic Press, San Diego) 1995.

[29] Kuga Y. and Ishimaru A., *J. Opt. Soc. Am. A*, **8** (1984) 831; van Albada M. P. and Lagendijk A., *Phys. Rev. Lett.*, **55** (1985) 2692; Wolf P. E. and Maret G., *Phys. Rev. Lett.*, **55** (1985) 2696.

[30] van Tiggelen B. A., *Phys. Rev. Lett.*, **75** (1995) 422; Rikken G. L. J. A. and van Tiggelen B. A., *Nature*, **381** (1996) 54.

[31] Sparenberg A., Rikken G. L. J. A. and van Tiggelen B. A., *Phys. Rev. Lett.*, **79** (1997) 757.

[32] John S., *Phys. Rev. Lett.*, **53** (1984) 2169; Anderson P. W., *Philos. Mag. B*, **52** (1985) 505; Dalichaouch R. *et al.*, *Nature*, **354** (1991) 53; Wiersma D. S. *et al.*, *Nature (London)*, **390** (1997) 671; Chabanov A. A. and Genack A. Z., *Phys. Rev. Lett.*, **87** (2001) 153901; Störzer M., Gross P., Aegerter C. M. and Maret G., *Phys. Rev. Lett.*, **96** (2006) 063904; van der Beek T., Barthelemy P., Johnson P. M., Wiersma D. S. and Lagendijk A., *Phys. Rev. B*, **85** (2012) 115401.

[33] Sapienza R., Costantino P., Wiersma D. S., Ghulinyan M., Oton C. and Pavesi L., *Phys. Rev. Lett.*, **91** (2003) 263902.

[34] Ghulinyan M., Oton C., Gaburro Z., Pavesi L., Toninelli C. and Wiersma D. S., *Phys. Rev. Lett.*, **94** (2005) 127401.

[35] Scheffold F. and Maret G., *Phys. Rev. Lett.*, **81** (1998) 5800.

[36] Bisi O., Ossicini S. and Pavesi L., *Surf. Sci. Rep.*, **38** (2000) 1.

[37] Schuurmans F. J., Vanmaekelbergh D., van de Lagemaat J. and Lagendijk A., *Science*, **284** (1999) 141.

[38] Akkermans E. and Montambaux G., *Mesoscopic Physics of Electrons and Photons* (Cambridge University Press) 2007.

[39] Martelli F., Contini D., Taddeucci A. and Zaccanti G., *Appl. Optics*, **36** (1997) 4600.

[40] Jackson J. D., *Classical Electrodynamics* (Wiley, New York) 1975.

[41] Vollhardt D. and Wölfle P., *Phys. Rev. B*, **22** (1980) 4666.

[42] Kuga Y. and Ishimaru A., *J. Opt. Soc. Am. A*, **8** (1984) 831; Albada M. V. and Lagendijk A., *Phys. Rev. Lett.*, **55** (1985) 2692; Wolf P. and Maret G., *Phys. Rev. Lett.*, **55** (1985) 2696.

[43] John S., *Phys. Rev. Lett.*, **53** (1984) 2169; Anderson P. W., *Philos. Mag. B*, **52** (1985) 505.

[44] Kaveh M. *et al.*, *Phys. Rev. Lett.*, **57** (1986) 2049.

[45] Wiersma D. S. *et al.*, *Phys. Rev. Lett.*, **74** (1995) 4193.

[46] Labeyrie G. *et al.*, *Phys. Rev. Lett.*, **83** (1999) 5266; Labeyrie G. *et al.*, *J. Opt. B - Quantum and Semiclassical Optics*, **2** (2000) 672; Bidel Y. *et al.*, *Phys. Rev. Lett.*, **88** (2002) 203902.

[47] Gurioli M. *et al.*, *Phys. Rev. Lett.*, **94** (2005) 183901.

[48] Freund I. *et al.*, *Phys. Rev. Lett.*, **61** (1988) 1214.

[49] Wiersma D. S., van Albada M. P. and Lagendijk A., *Phys. Rev. Lett.*, **75** (1995) 1739.

[50] Vlasov D. V. *et al.*, *Pisma Zh. Eksp. Teor. Fiz.*, **48** (1988) 86 (*JETP Lett.*, **48** (1988) 91).

[51] Kuzmin L. V., Romanov V. P. and Zubkov L. A., *Phys. Rev. E*, **54** (1996) 6798.

[52] Koenderink A. F. *et al.*, *Phys. Lett. A*, **268** (2000) 104; Huang J. *et al.*, *Phys. Rev. Lett.*, **86** (2001) 4815.

[53] van Tiggelen B. A., Lagendijk A. and Wiersma D. S., *Phys. Rev. Lett.*, **84** (2000) 4333.

[54] Abrahams E., Anderson P. W., Licciardello D. C. and Ramakrishnan T. V., *Phys. Rev. Lett.*, **42** (1979) 673.

[55] John S., *Phys. Rev. Lett.*, **53** (1987) 2169.
[56] Bliokh K. Y., Bliokh Y. P., Freilikher V., Genack A. Z., Hu B. and Sebbah P., *Phys. Rev. Lett.*, **97** (2006) 243904.
[57] Bertolotti J., Galli M., Sapienza R., Ghulinyan M., Gottardo S., Andreani L. C., Pavesi L. and Wiersma D. S., *Phys. Rev. E*, **74** (2006) 035602.
[58] Bertolotti J., Gottardo S., Wiersma D. S., Ghulinyan M. and Pavesi L., *Phys. Rev. Lett.*, **94** (2005) 113903.
[59] Atwater H. and Polamn A., *Nat. Mater*, **9** (2010) 205.
[60] Pitarke J. M., Silkin V. M., Chulkov E. V. and Echenique P. M., *Rep. Prog. Phys.*, **70** (2007) 1.
[61] Fahr S., Rockstuhl C. and Lederer F., *App. Phys. Lett.*, **95** (2009) 121105.
[62] Schaadt D. M., Feng B. and Yu E. T., *App. Phys. Lett.*, **86** (2005) 063106.
[63] Nishijima Y., Rosa L. and Juodkazis S., *Opt. Express*, **20** (2012) 11466.
[64] Mupparapu R., Vynck K., Malfanti I., Vignolini S., Burresi M., Scudo P., Fusco R. and Wiersma D. S., *Opt. Lett.*, **37** (2012) 368.